NASA/CP—2001–209986

2001 Flight Mechanics Symposium

Edited by
John P. Lynch
NASA Goddard Space Flight Center
Greenbelt, Maryland

Proceedings of a conference sponsored and held at
NASA Goddard Space Flight Center
Greenbelt, Maryland
June 19–21, 2001

June 2001

CALIBRATION OF HUBBLE SPACE TELESCOPE FOCAL-LENGTH VARIATIONS USING THE EMBEDDING TECHNIQUE

Lee Barford, Nicholas Tufillaro and Daniel Usikov
Agilent Laboratories, Systems and Solutions Lab

Leonid Marochnik and Robert McCutcheon
Computer Sciences Corporation / Space Telescope Science Institute

ABSTRACT

A modeling method that allows one to rapidly build data-driven models of nonlinear components is discussed. The models are constructed from input/output time domain data and their "embeddings". The notion of models built from embedded data is described in the Taken's Embedding Theorem and has been extensively explored for modeling systems in the physics literature. The authors from Agilent Laboratories are developing practical methods to extend these results to non-autonomous systems by creating tools that allow engineers to rapidly build models for driven nonlinear components. These models can be used in simulation, process control, diagnostics, and sensor calibration.

Using these methods a "black-box" data-driven model is generated to calibrate Hubble Space Telescope (HST) focal-length changes on a 5-minute time grid for the period from 1995-1999. These models are built using a program, CHAOS, developed by Agilent Laboratories. The data-driven model predicts the focus for the measured points about 36 percent better than the Full-Temperature Model (FTM) constructed from a detailed knowledge of the telescope structure. As demonstrated by this HST focal-length calibration, data-driven models, such as those generated with the CHAOS package, have great potential for application to a wide spectrum of HST/Next Generation Space Telescope (NGST) calibration problems. In particular, for sensor calibration applications, black-box nonlinear models can be generated rapidly, which have similar or better performance than models built from a detailed understanding of the system structure.

1. INTRODUCTION

This paper describes a nonlinear data-driven "black-box'' model of HST focus behavior at 5-minute intervals for the period 1995-1999. The model uses techniques originally developed in "chaos theory'' for describing the behavior of nonlinear dynamic systems based only on observed data. A short description of this model can be found at the top of each quarter-year file on the HST website:

http://www.stsci.edu/instruments/observatory/focus/ephem.html

This paper contains no information about the HST framework and optical telescope assembly as related to thermal effects on the telescope focal length. A comprehensive description of these systems and thermal effects can be found in the paper [1], which also describes three physics based models – the Four-Temperature Model, the Attitude Model, and the Full-Temperature Model – created by John Hershey[1]. We do not discuss these models here, nor do we discuss their comparative pros and cons with respect to the black-box data-driven model from the physical point of view. We do, however, discuss the comparative fits of the various models to the focus measurement data, and we compare model prediction characteristics at times between focus measurements.

We use the CHAOS Program (CP) to rapidly develop a nonlinear black-box model. We refer to this black box model as the Chaos Program Model (CPM) when comparing this model to previously developed models such as FTM. The general approach and method used to build these data-driven models is described in Section 2. Section 3 provides a brief description of what the CP is and how it works. Section 4 of this paper provides additional details about data files used and the models constructed.

One of the goals of this paper is to demonstrate the applicability of black-box modeling using embedding techniques to spacecraft sensor calibration problems. By *black box*, we mean a model that requires no deep information about the device (i.e., science instrument, fixed-head star tracker, etc., to be calibrated) be known before model building. The nonlinear model extraction behind our methods is based on the so-called *dynamic-reconstruction theory*, which is described in Section 2. This theory of nonlinear system identification is based on the Taken's Embedding Theorem, which very roughly states that the evolution of points in the "reconstructed" state space of our data-driven model can be related by a change of variables to that of actual dynamics (a first principles model) believed to be determining the systems motion. Thus, the embedding theorem opens the way toward a general solution for extracting black-box models for nonlinear devices directly from time-domain measurements. We selected the HST focus calibration task for this initial demonstration project because of easy access to focus data and the existence of focus models developed using more traditional methods.[1]

We found that across the period from 1995 through early 1999, the black-box model fits the observed focus data better than the existing Four-Temperature, Attitude, and Full-Temperature models. The root-mean-square (RMS) residuals for the CPM show 42 percent, 48 percent, and 36 percent improvements over the residuals for the three existing models (see details below).

Figure 1a shows focus observations along with FTM and CPM focus predictions from 1995 through the first quarter of 1997 [mostly before HST servicing mission 2 (SM2)]. Figure 1b plots the same data from the second quarter of 1997 through the first quarter of 1999. These two figures demonstrate how well the FTM and the CPM predict the observations.

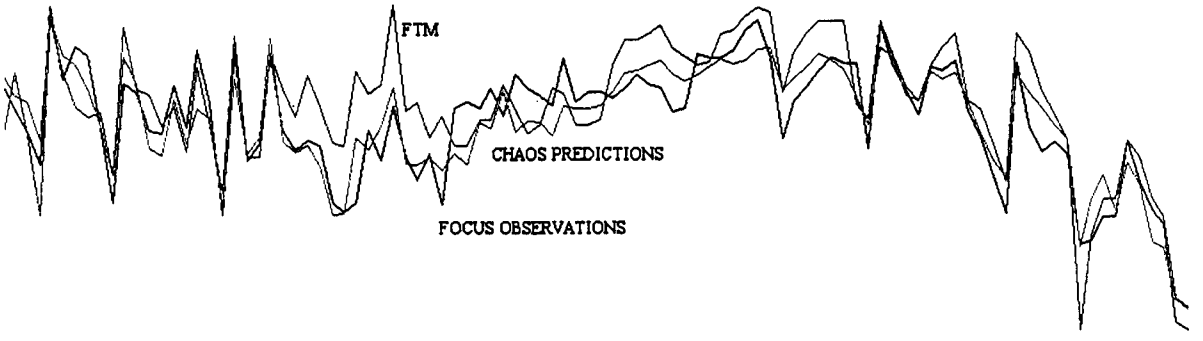

Figure 1a. Focus Observations and FTM and CPM Focus Estimates From 1995 Through First Quarter of 1997 (Mostly Before SM2). The Chaos Program prediction is 29.3% better than FTM.

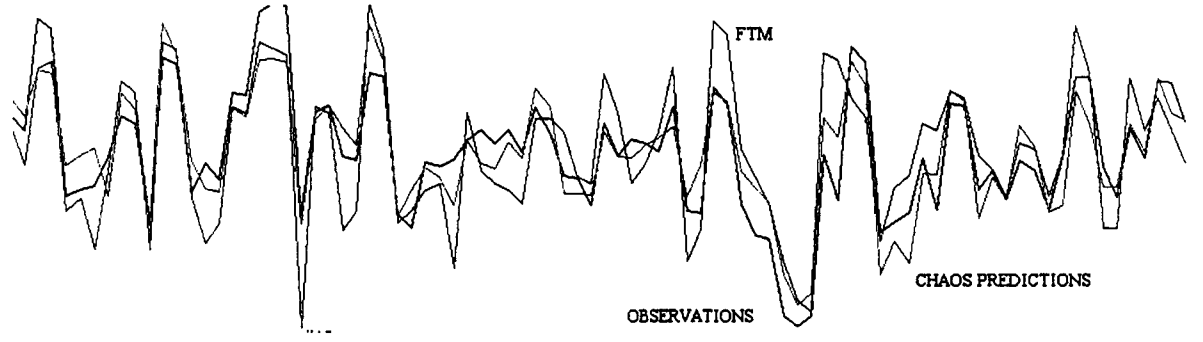

Figure 1b. Focus Observations and FTM and CPM Focus Estimates From Second Quarter of 1997 Through First Quarter of 1999 (Mostly After SM2). The Chaos Program prediction is 36% better than FTM.

---

[1]An HST web site presents the focus data for these models at 5-minute intervals for each quarter of each year from 1994 through 1999. John Hershey provided us with raw temperature data for the same time period.

2. "DYNAMIC RECONSTRUCTION THEORY" for SENSOR and SYSTEM CALIBRATION

If a system is well described by linear theory, then a transfer function can be used for building data driven models for the system [2]. Nonlinear systems, especially those that are not weakly nonlinear, require a different approach. Some methods that have been developed to model and calibrate nonlinear systems include Volterra Series, neural nets, and cluster weighted models to name a few [3]. Here we are concerned with models that are constructed only from input/output data, and which require very little system specific information. The advantage of such data driven models and calibration systems is that they can be developed much more rapidly than detailed first principle models. The disadvantage of such data driven models is that they may require extensive data sets for model training and they typically will have poor extrapolation properties (as an attempt to predict the system's behavior out of the training box of inputs).

A dynamical systems approach to "black box" modeling was first suggested by Casdagli [4] (see [5]). Using time domain input/output data, an attempt is made to embed the original data in a higher dimensional space, built from transforms of the original data of sufficient dimension so that the determinism of the dynamical system is recovered. This approach to nonlinear system identification is sometimes called "Dynamic Reconstruction Theory" [6] and begins with a state space representation of the form

$$\dot{x} = f(x(t), u(t)); \quad y(t) = h(x(t)); \tag{1}$$

or a numerical version of difference equations,

$$x_{n+1} = f(x_n, u_n). \tag{2}$$

In these equations f, x, u are typically vectors and $u(t)$ is the input, drive, or stimulus, $x(t)$ is the state, and $h(t)$ is a measurement function.

Attempts to build the state space models appear hard on at least two counts: first, without any specific form for a model the relevant dynamical variables, x, appear to be unknown, and second, even if one knows what variables are needed to be included, they still may not be accessible to experimental measurements. Both of these issues, essentially the nonlinear order, or dimension of the model, and model selection and calibration are discussed below.

A simple approach to nonlinear modeling in the time domain could begin by plotting the input and output on a graph. Next we could create a function from the stimulus, $u(t)$, to the response $y(t)$,

$$y(t) = F[u(t)]; \tag{3}$$

but this function might not be unique. As seen in Figure 2, for example, two different inputs can have the same output. However, the slope at each of these input points is different. So an "embedded" input variable created from a vector formed by the input and its derivative does have a unique output in this example.

A key insight of dynamic reconstruction is thus to embed the measured variables to resolve any indeterminacy by building a function not just with $y(t)$, but also transforms of y, for example its numerical derivatives. In more general terms, an "embedding" is a map that places an "m" dimensional manifold, in this case a one-dimensional curve, in a higher "n" dimensional space. We then attempt to build input/output models not based on the measured scalar data, but rather maps on vectors of embedded data.

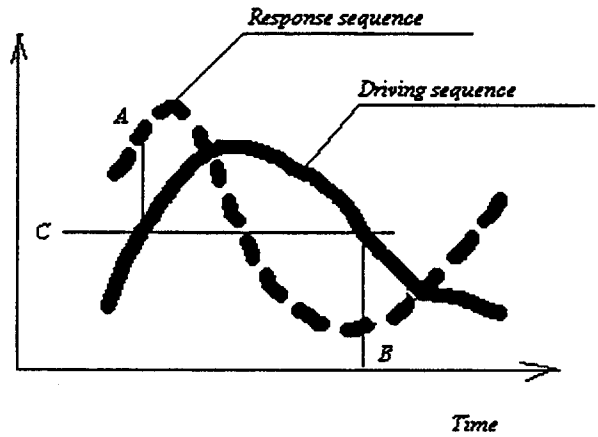

Figure 2. Embedding: Effect of Driving Sequence on Response Sequence

One simple class of models would be a polynomial model that could be of the form,

$$y(t) = a_0 + a_1 u + a_2 \dot{u} + a_3 u\dot{u} + a_4 u^2 + a_5 \dot{u}^2 ...; \tag{4}$$

The unknown coefficients ($a_0, a_1, a_2, ...$) can be determined by least squares. Plotting the embedded trajectory in the enlarged phase space can untangle and remove the indeterminacy. This idea can also be applied to difference equations as well,

$$f(n+1) = F[f(n)] \tag{5}$$

and in effect create a numerical approximation for the differential equations generating the flow.

Due to a theorem of Taken's (with an extension to the driven case by Stark [5]) these embedded models are diffeomorphic to the dynamics of the original system. This means that there is a continuous and differentiable map from the original system trajectory to the new embedded system (created from the measured variables) of sufficient dimension. In particular, deterministic prediction is possible from an embedded model that will mimic the actual dynamics.

Thus, embedding opens the way toward a general solution of extracting black box models for the observable dynamics of nonlinear systems directly from input/output time series data. It can solve the fundamental existence problem, however, the gulf between these theoretical results and practical implementation is wide.

In most of the research physics literature, the components' behavior is described by embedding both the inputs and outputs in the form

$$z(t) = G[y(t-\tau), y(t-2\tau), ..., y(t-l\tau), u(t), u(t-\tau), ..., u(t-(k-1)\tau)] \tag{6}$$

where G is fitted to the data using nonlinear modeling methods such as global polynomials, neural nets, or radial basis functions [3]. The form of the equations shows a "lag" embedding with a time delay, τ, input lag dimension, k, and output lag dimension, l, though in practice one can find that better quality models can often be built using other embeddings such as linear transforms, integral and differential transforms, and wavelets to help bring out the salient dynamical features in the data.

Given the above model form, the problem now reduces to a number of technical issues such as: Determination of the dimensions (k and l), determination of lags (τ) or other forms of embeddings and embedding parameters,

determination of model class G, and fitting the model parameters, model validation, and design of excitation signals (where possible) for a given model/signal class.

It might be helpful to point out that this relation between a continuous dynamical system and an embedded model built from time-delayed input/output signals can be made explicit in the case of linear systems. The details for an algorithm are described by Franklin [7], which shows how to go from the linear system with matrices A, B, and C to a model based only on delayed variables. Unfortunately, no explicit constructive proof exists for nonlinear systems.

For embeddings built from a time delay lag, τ,

$$y(t) = G[y(t-\tau),...,y(t-l\tau),u(t),u(t),...,u(t-(k-1)\tau)] \tag{7}$$

we can use an extension of the algorithm for the theory of embedded autonomous systems known as ``False Nearest neighbors" [8], [9]. The smallest "k" and "l" can be found by creating a statistic that checks if vectors close in a delay space are also close in a delay space of greater dimension. If they are not, they are the false neighbors and G is not single valued. This diagnostic is independent of G.

For models built from time delays, one should estimate the time lag value, τ. Again, a diagnostic can be used from the theory of autonomous systems. The mutual information or the first zero of the autocorrelation function [8] work well. In cases where there is a single dominant frequency band, both of these diagnostics often turn out to be about one-quarter of the dominant frequency. In other words, τ is chosen so that the delay variables are decorrelated as much as possible. In practice, though, these diagnostics are not nearly so useful as software tools such as the Chaos Program that allows one to rapidly build and test models with different combinations of embedding functions and parameters.

Once a suitable embedding is found, the next task is to find the function approximation of G. We try to keep things here as simple as possible. First we usually try a global polynomial fitted by least squares. For other applications we have had some success with radial basis functions

$$y = \alpha + \beta u + \sum_{i=1}^{N} \omega_i \phi(\| c_i - u \|) \tag{8}$$

that use optimization algorithms which can automatically determine the number and placement of the basis functions [10]. We found that the neural net approach sometimes works better on extrapolation than the polynomial-based methods, but the neural net requires much more time for building and verifying the created models.

With software tools such as the CP, one can rapidly test out different basis functions and model structures. For validation, i.e. testing the models on overfitting and underfitting, simple cross validation methods are sufficient in the examples we consider here. That is, models are only built from a subset of the available data (the training set), and then tested on the remaining data.

3. CHAOS PROGRAM

The CP uses embedded signals to build models as described in Section 2. The program provides a graphical user interface with tools that assist the user with importing, inspecting, and analyzing data. Next the program allows the user to create various data embeddings, and finally to fit and evaluate models based on the embedded data. For the models considered here the initial input data can be described as a time series of drive and response variables, and embeddings created from the drive variables, such as their numerical derivatives.

To create models, the input and output data are fitted with a polynomial, as in the following equation:

$$f_{response} = x_0 + x_1 f_{drive} + x_2 \dot{f}_{drive} + x_3 f_{drive} \dot{f}_{drive} + x_4 \left(\dot{f}_{drive}\right)^2 + ... \tag{9}$$

The ''embedded'' derivative variables are calculated numerically from the measured drive data. The unknown coefficients $(x_0, x_1, x_2, x_3, x_4, \ldots.)$ of the polynomial are found by a least squares methods (LSM) on the training sequence and are then used for prediction.

Thus, the problem solved is a construction of a black box behavioral model for an object with nonlinear behavior (a polynomial of degree higher than one) describable by a functional or differential relation among the state variables. Complete documentation for the program and more details about the CP can be found in the Chaos User's Manual by Usikov [11].

The accuracy of any data-driven model is restricted by the amount of noise in the source data and the accuracy of the computation. The latter can be mitigated by improved computation technique (i.e., by double precision, robust algorithms, etc.). However, the experimental accuracy often cannot be improved. This is one reason why the embedding technique has inherent limitations. Also, these techniques are limited to systems that can be effectively described by only a few dimensions, i.e., embedding variables. This limitation is not as harsh as might first appear since dissipation in even a very complex system can greatly reduce the effective degrees of freedom, the number of modes actually excited. Additional difficulties arise when the data to be modeled have many different time-scales. For these systems additional embedding strategies, such as using wavelet embedding, are very useful. A wavelet embedding algorithm is implemented in the Chaos program and can be explained using the following example. Consider a wavelet with width = 3. The embedding value derived from a source variable is calculated on six sequential points in time: $I_6 = f_6 + f_5 + f_4 - f_3 - f_2 - f_1$. It is a kind of averaged first derivative (i.e., the derivative, which is smoothed over a span of points).

By averaging the data in this way we can create new embedded variables that are more in tune with longer time constants.

4. CHAOS PROGRAM MODEL

To build an HST focus model, we could use any of the data used to create the three already existing models. The first of these, the Four-Temperature Model, is based on four temperature sensors in the light shield near the secondary mirror spider. The second model, the Attitude Model, is based on HST attitude information from the mission scheduler files (Sun angles, off-nominal rolls, occultations, and day/night satellite positions). The third model, the Full-Temperature Model (FTM), is based on a large number of temperature sensors throughout the telescope, including the four sensors in the first model. Because the FTM represents the observations somewhat better than the other two models do, we chose to use the raw data used to create the FTM to build the CPM.

Table 1 shows an extraction from the typical raw data file (from the first quarter of 1997) used to build the CPM.

Table 1. Sample From Raw Data File

Year	Day	Hour	Min.	Julian Date	Temperature Functions (degrees Celsius)						Observed Focus Position (microns)
					T1	T2	T3	T4	T5	T6	
1997	9	22	20	50457.92969	28.8	-9	-24.1	-8.4	-37.3	16.8	
1997	9	22	25	50457.93359	28.6	-8.8	-23	-8.6	-36	16.8	
1997	9	22	30	50457.93750	28.8	-9	-22.7	-8.5	-34	16.8	
1997	9	22	35	50457.94141	28.8	-9	-21.7	-8.1	-32.7	16.8	
1997	9	22	40	50457.94531	28.7	-9.2	-21.2	-8.1	-31.5	16.8	
1997	9	22	45	50457.94922	28.8	-9	-20	-7.9	-30.5	16.8	
1997	9	22	50	50457.95313	28.8	-9	-19.3	-7.8	-30.4	16.8	3.00E-01
1997	9	22	55	50457.95703	28.8	-9	-19.1	-7.6	-30.6	16.7	9.00E-01
1997	9	23	0	50457.96094	28.7	-9.2	-19	-7.4	-30.9	16.8	
1997	9	23	5	50457.96094	28.7	-9	-19.7	-7.4	-31.5	16.8	
1997	9	23	10	50457.96484	28.8	-9	-20.5	-7.4	-32.5	16.8	

T1, T2, T3, T4, T5, and T6 are six functions of many telescope temperature sensors, including four light shield temperatures near the secondary mirror; each function is the mean of a number of sensor measurements extracted by the Observatory Monitoring Program:

- T1: Truss axial temperature difference function
- T2: Truss diametrical temperature difference function
- T3: Aft shroud temperature function
- T4: Forward shield temperature function
- T5: Light shield temperature function
- T6: Primary mirror temperature function

The last column of the table contains focus position observations; in most cases, the value shown in this column is blank, indicating that no observations were made for the corresponding time row. The focus observations are measured in units of secondary mirror microns and are relative to the best focus (zero microns) of the wide field planetary camera 2 (WFPC2)[2]

We have excluded from consideration the focus measurements of 1994 and four focus observations of 1995 and 1996 because no regular temperature data (T1-T6) exist for the appropriate times. Consequently, we are dealing with a typical calibration task: using existing focus observations and appropriate raw data (T1-T6) for the time of

[2] According to convention (see http://www.stsci.edu/instruments/observatory/focus/focus2.html), we express all focus changes in the science instrument-independent units of secondary mirror microns. A +1-micron change is equivalent to a physical movement of the secondary mirror by that amount away from the primary mirror. One micron of secondary mirror defocus translates to 110 microns at the focal plane. The focus zero point is defined as WFPC2 best focus as determined by point spread function (PSF)-fitting (phase retrieval) software for PSFs in the ~400-800 nanometer range.

observations to predict focus values for time rows with no observations. To do that, we must create the focus model using the existing set of observations.

We have divided all focus observations into two data sets. The first data set, mostly before SM2, includes the time period from 1995 to the first quarter of 1997 and contains 98 observations. The second data set, after SM2, includes the time period from the second quarter of 1997 to the first quarter of 1999 and contains 86 observations.

By experimenting, we have found one transfer function (embedding scheme) that applies equally well to both data sets. It uses the following terms: a constant offset; modified Julian date; temperature functions T1, T4, and T5; three-point wavelets of T1, T4, and T5; and the first derivative of T5:

$$F_E = C_0 + C_1 t + C_2 T1 + C_3 W(T1) + C_4 T4 + C_5 W(T4) + C_6 T5 + C_7 W(T5) + C_8 \frac{\Delta T_5}{\Delta t}$$

where

$$\begin{aligned} F_E &= \text{focus estimate (microns)} \\ t &= \text{modified julian date} \\ W(T) &= \text{three-point wavelet function of temperature function T} \\ \frac{\Delta T5}{\Delta t} &= \text{first derivative approximation for } T_5 \\ &= (T5(t_2) - T5(t_1))/(t_2 - t_1) \\ C_1 \cdots C_9 &= \text{polynomial coefficients} \end{aligned}$$

Calculations show that including T2, T3, and T6 in the transfer function does not improve the fit.

Note that the sensitivity to three-point wavelets means that the current value of the focus depends on the nearest time history of temperatures before the focus observation. The three-point wavelet uses six points of data; for a 5-minute time grid, this equals 25 minutes, about one-fourth of the orbital period for HST. The temperature inertia of the sensors might be responsible for this result.

We have computed two sets of transfer function coefficients (one for data set one and one for data set two), and we have used these to evaluate the fit to the observed focus measurements. Table 2 shows standard deviations from focus observations for the Four-Temperature, Attitude, Full-Temperature, and Chaos Program Models. In the first column, the notations 95_1, 97_2, etc., mean first quarter of 1995, second quarter of 1997, etc. One can see from Table 2 that the CPM fits the observed focus data points better than the existing Four-Temperature, Attitude, and Full-Temperature models.

Figure 3 gives an overview of data for the first quarter of 1997. It shows the behavior of all functions of interest with 5-minute time intervals. From this figure one can see the behavior of all three temperature functions (T1, T4 and T5), estimates of all four models, and observations. Note the drop in the CPM focus estimates at a time when there is a jump in several of the temperature functions.

Recall that only 184 observed focus measurements were available to construct the focus models. Fortunately, this is sufficient to conduct a statistical test to check inconsistencies in estimated focus amplitudes for the different models. One can plot a histogram of the number of measured foci in an interval of focus values vs. the focus value. Assuming that the focus measurement is a random process (in time) and that the typical time interval of focus variation is much smaller than the time between focus measurements, such a histogram, calculated on the set of measured points only, would be similar to the histogram calculated if exact focus values were known for all times. The model whose histogram is closest to the measured focus histogram should be the more statistically acceptable model.

Table 2. Standard Deviations (microns)

Year_ Quarter	Four-Temp. Model	Attitude Model	Full-Temp. Model	Chaos Program Model	Number of Focus Observations	Comments
95_1	1.312	1.310	1.068	0.584	6	
95_2	2.2	2.2	2.2	0.56	1	
95_3	1.444	0.850	1.196	0.974	4	
95_4	1.116	1.113	0.775	0.693	6	One observation has been removed
96_1	0.995	1.603	0.789	0.780	3	One observation has been removed
96_2	0.913	1.294	0.469	0.446	3	Two observations have been removed
96_3	1.522	2.033	1.570	0.877	8	
96_4	1.917	1.354	1.577	1.015	8	
97_1	1.222	1.134	0.848	0.726	59	
97_2	1.186	1.268	1.078	0.919	16	
97_3	1.822	1.952	1.647	1.003	10	
97_4	0.925	0.753	0.870	0.664	8	
98_1	1.074	1.312	0.832	0.664	11	
98_2	1.917	2.765	1.967	0.940	18	
98_3	1.600	1.512	1.304	0.780	10	
98_4	0.685	1.251	0.699	0.844	10	
99_1	0.519	1.173	1.266	0.472	3	
Average Standard Deviation:	1.316	1.463	1.186	0.761	184	

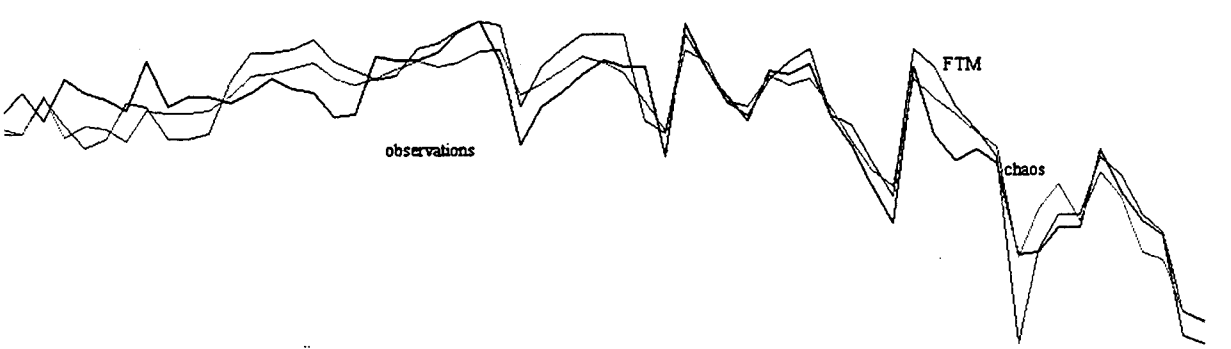

Figure 3. Overview of Focus Model Behavior for First Quarter of 1997. FTM and Chaos Program standard deviations are 0.848 and 0.720, respectively.

Figures 4 and 5 show the histograms. Figure 4 gives frequencies (absolute numbers) of amplitudes predicted by the CPM and the FTM that can be compared with the frequencies of amplitudes found for focus observations. This histogram takes into account all 184 focus measurements and the corresponding estimates from the CPM and the FTM. A comparison of the statistics shows that the CPM estimates are closer than the FTM estimates to the observed frequencies.

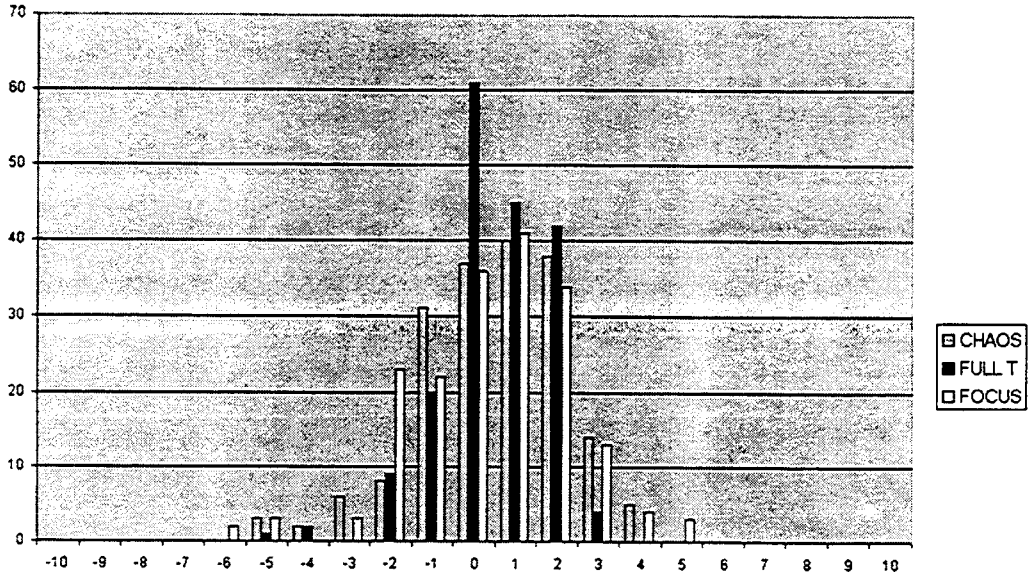

Figure 4. Frequencies of Amplitudes (in Microns) Predicted by CPM and FTM in Comparison With Frequency of Amplitudes Found for Focus Observations (Observational Points Only)

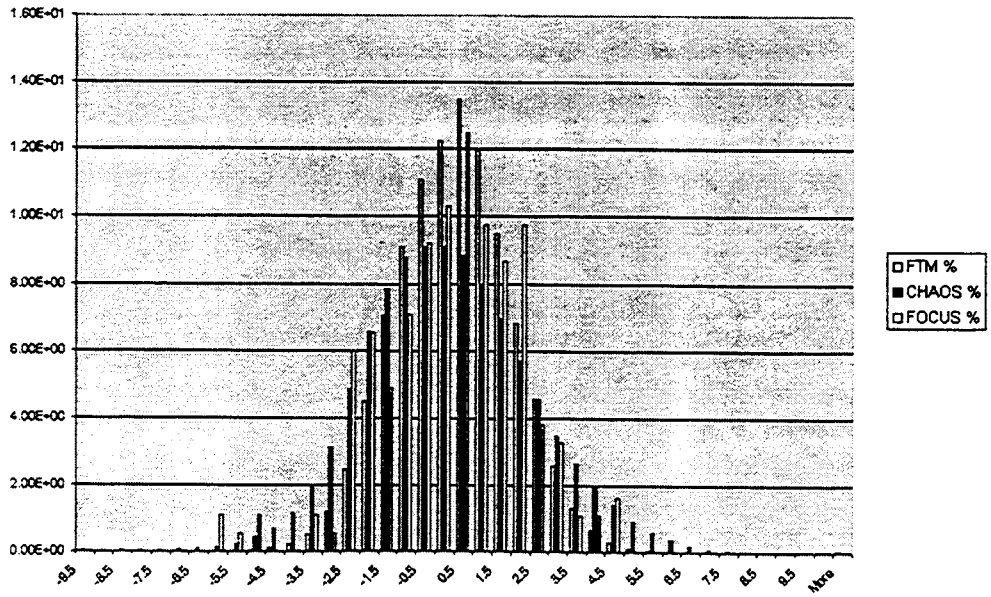

Figure 5. Frequencies of Amplitudes (in Microns) Predicted by CPM and FTM in Comparison With Frequency of Amplitudes Found for Focus Observations (All Points With 5-Minute Grid)

One can see that the FTM overestimates small amplitudes and underestimates large ones. As a result, when time profiles of focus estimates are overlapped, it appears (but only appears) as though the CPM is overestimating large amplitudes.

Figure 5 is similar to Figure 4. The only difference is that the estimates of focus amplitude from the CPM and the FTM are for all points (i.e., for all points on the 5-minute time grid, not just the 184 observation points). This figure confirms that the CPM is closer than the FTM to the observed focus distribution in the region of large amplitudes.

5. CONCLUSION

The CPM fits the focus observations somewhat better than existing physical models do in terms of both achieved LSM deviation on the measured points and the histogram statistics. We expect that the fit could be improved even more if the additional available data (i.e., the four light shield temperatures and the attitude parameters) are taken into account. Perhaps more importantly, the time to develop and verify a data-driven model can be significantly less than other approaches.

We expect also that the Chaos Program or similar software could be successfully used for the calibration of other HST/NGST science instruments and devices. Using embedding variables that capture the appropriate time scales of interest in the data before performing an LSM fit is a key step that allows the creation of accurate data-driven models.

REFERENCES

1. Hershey J., 1997. Space Telescope Science Institute (STScI) document SESD-97-01, http://www.stsci.edu/instruments/observatory/focus/focus2.html
2. Rugh W. J., 1996. Linear System Theory, Prentice Hall, NJ.
3. Gershenfeld Neil A. 1999. The Nature of Mathematical Modeling, Cambridge University Press.
4. Casdagli M. 1992. Dynamical systems approach to modeling input-output systems, Nonlinear Modeling and Forecasting, SFI Studies in the Sciences of Complexity. In: Proc. Vol XII, Eds. M. Casdagli and S. Eubank, Addison-Wesley.
5. Stark J., 1999. Delay embeddings and forced systems, *J. Nonlinear Science*, 9, 255-332
6. Haykin S., Principe J., 1998. IEEE Signal Processing Magazine, p. 66-81.
7. Franklin G. F., 1994. Feedback control of dynamic systems, Addison-Wesley.
8. Kantz H., Schreiber T., 1997. Nonlinear time series analysis, Cambridge University Press.
9. Walker David M., Tufillaro Nicholas B. 1999. Phase-space reconstruction using input-output time series data, *Phys. Rev. E* 60 (4), 4008-4013.
10. Walker David M., Brown Reggie, Tufillaro Nicholas B. 1999, Constructing transportable behavioral models for nonlinear electronic devices, *Phys. Letts A* (255) 4-6, 236-242.
11. Usikov D., 1999. Chaos Program Users Manual, Agilent Technologies (unpublished)